ELSEVIER

Chemosphere 62 (2006) 926–933

CHEMOSPHERE

www.elsevier.com/locate/chemosphere

Degradation mechanism and the toxicity assessment in TiO_2 photocatalysis and photolysis of parathion

Tak-Soo Kim [a], Jung-Kon Kim [a], Kyungho Choi [a], Michael K. Stenstrom [b], Kyung-Duk Zoh [a,*]

[a] *Institute of Health and Environment, School of Public Health, Seoul National University, Seoul 110-799, Republic of Korea*
[b] *Department of Civil and Environmental Engineering, University of California, Los Angeles, CA 90095, USA*

Received 17 January 2005; received in revised form 21 May 2005; accepted 24 May 2005
Available online 26 July 2005

Abstract

The photocatalytic degradation of methyl parathion was carried out using a circulating TiO_2/UV reactor. The experimental results showed that parathion was more effectively degraded in the photocatalytic condition than the photolysis and TiO_2-only condition. With photocatalysis, 10 mg/l parathion was completely degraded within 60 min with a TOC decrease exceeding 90% after 150 min. The main ionic byproducts during photocatalysis were measured. The nitrogen from parathion was recovered mainly as NO_3^-, NO_2^- and NH_4^+, 80% of the sulfur as SO_4^{2-}, and less than 5% of the phosphorus as PO_4^{3-}. The organic intermediates 4-nitrophenol and paraoxon were also identified, and these were further degraded. Two different bioassays (*Vibrio fischeri* and *Daphnia magna*) were used to test the acute toxicity of solutions treated by photocatalysis and photolysis. A Microtox test using *V. fischeri* showed that the toxicity, expressed as the relative toxicity (%), was reduced almost completely after 90 min under photocatalysis, whereas only an 83% reduction was achieved with photolysis alone. Another toxicity test using *D. magna* also showed that the relative toxicity disappeared after 90 min under photocatalysis, whereas there was a 65% reduction in relative toxicity with photolysis alone. The pattern of toxicity reduction parallels the decrease in parathion and TOC concentrations.

Keywords: Mineralization; 4-Nitrophenol; Paraoxon; Microtox; EC_{50}; *Vibrio fischeri*; *Daphnia magna*

1. Introduction

Organophosphorus pesticides are widely used in agriculture and industry (Dzyadevych and Chovelon, 2002). Parathion (methyl parathion, CAS No. 56-38-2) is a non-systemic insecticide that is used in many countries worldwide. It is used as a fumigant and acaricide and as a pre-harvest soil and foliage treatment for a wide variety of crops, both outdoors and in greenhouses (WHO, 2004). It is acutely toxic to mammals, acting by inhibiting the enzyme acetylcholinesterase (AChE) in nerve tissue. Parathion is classified as an acutely toxic pesticide by the US EPA (2003). Fig. 1 shows the chemical structures and UV spectra of methyl parathion and its environmental degradation byproducts: methyl paraoxon and 4-nitrophenol.

For treating parathion residues in water, biological and physical processes such as wetland and thermal decomposition have limitations due to their land and

* Corresponding author. Tel.: +82 2 740 8891; fax: +82 2 745 9104.
E-mail address: zohkd@snu.ac.kr (K.-D. Zoh).

0045-6535/$ - see front matter © 2005 Elsevier Ltd. All rights reserved.
doi:10.1016/j.chemosphere.2005.05.038

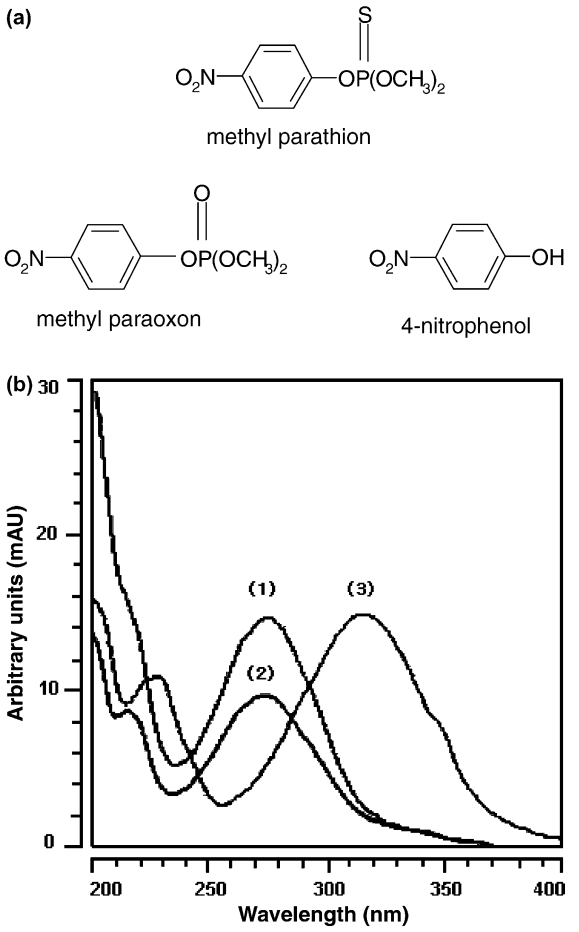

Fig. 1. (a) The chemical structures and (b) UV spectra of methyl parathion (1) and its degradation byproducts: methyl paraoxon (2) and 4-nitrophenol (3).

energy constraints (Germain et al., 2000; Schulz et al., 2003). There is a pressing need for a readily available economical, on-site, low energy technology for this purpose. Advanced oxidation processes (AOPs) have been proposed as an alternative for the treatment of wastewater. Of particular interest is the use of TiO_2 as a heterogeneous semiconductor catalyst, with solar light as the energy source (Malato et al., 2003). One of the potential advantages of this process is that photocatalysis can completely mineralize a variety of aliphatic and aromatic compounds under suitable conditions.

The degradation of parathion using TiO_2 photocatalysis was recently investigated (Doong and Chang, 1998; Konstantinou et al., 2001; Konstantinou and Albanis, 2003). These studies focused on the kinetics and the identification of intermediates. However, the degradation mechanism and the toxicity of the treated water were not investigated.

Successful treatment of a pollutant by TiO_2 photocatalysis must address the disappearance of the parent compound as well as identification of the intermediates and end-products to insure that harmful or toxic end-products are not produced. The toxicity of known end-products may be determined from literature surveys, but in the case of unknown end-products, a battery of different bioassays using organisms from different trophic levels can be used to insure that the end-products are not harmful.

This paper focuses on the kinetics, mechanisms and the end-product toxicity of parathion degradation in water using TiO_2 and artificial UV light. Parathion degradation rates were compared for TiO_2-alone, photolysis (UV-only) and photocatalysis (UV and TiO_2). The mechanism of the photocatalytic degradation of parathion is discussed by referring to the analysis of intermediates, byproducts, and TOC. Also, two different bioassays were performed to evaluate the toxicity of the treated water after photocatalysis and photolysis, and these results were compared with measurements of the byproducts and TOC. Toxicity was measured at different stages of parathion degradation using a modified Microtox 81.9% test using *Vibrio fischeri* (*V. fischeri*) and a 48-h acute toxicity test using *Daphnia magna* (*D. Magna*).

2. Materials and methods

2.1. Chemicals

Methyl parathion (99.4%), methyl paraoxon (98.3%), and 4-nitrophenol (99%) were purchased from Chem Service. TiO_2 (Degussa P-25, with a BET surface of $50 \pm 15\ m^2/g$) was used with no pre-treatment. All other reagents were of analytical grade and were used without further treatment.

2.2. Photoreactor

The photocatalytic degradation experiments were performed in a circulating photoreactor system. The reactor system consisted of a temperature-controlled reservoir consisting of a stirred 2 l glass bottle, a metering pump (Cole-Parmer, Chicago, IL) for circulating the reactor contents, and a photoreaction chamber, all of which were connected with flexible Teflon tubing. The parathion solutions were continuously recirculated with a rotary pump (Master Flex 7592-50, Cole-Parmer) at a flow rate of 1 l/min. Reactor stirring was sufficient to maintain uniformity of the reaction solution.

The UV chamber consisted of six UV-A lamps (Sankyo Electrics Co., 20 W, 365 nm) and six quartz columns (10 mm diameter, 650 mm length). The distance from a UV lamp to a quartz column was 20 mm. The light intensity was measured using a Radiometer (VLX-3 W Radiometer 9811-50, Cole-Parmer) at 365 nm (UV-A

region). The intensity of a single UV lamp measured at a distance of 20 mm was 2.4 mW/cm^2. The external surface of the reactor around the quartz columns was covered with aluminum foil for UV safety and energy consideration.

Reactions were performed under atmospheric pressure at 20 °C. The reaction solutions were prepared by diluting stock solutions and the aqueous phase was then introduced into the reservoir. The initial pH of the reaction solution was measured by a pH meter (PerpHect 330, Orion) and then adjusted to 7.0 (±0.4) with small amounts of 1 N HCl and 1 N NaOH. The reaction solution was transferred to the sample collector and solution storage vessel using a 3-way valve.

2.3. Analysis

All the liquid samples were first filtered through 0.2 μm PTFE (polytetraflouroethylene) membrane disposable filters (Advantec MFS Inc., Pleasanton, CA) to remove the TiO_2 particles before analysis. Parathion and its intermediates were determined by a Summit™ HPLC system (Dionex), equipped with an UVD340S detector, and RP C-18 silica column (25 cm × 4.6 mm i.d., 5 μm particles, Supelco Park). The eluent system of acetonitrile/water were used to run the chromatography in gradient mode; first 4 min with acetonitrile:water (40:60), and a linear gradient for 2 min to acetonitrile:water (70:30), holding for 4 min, then back to acetonitrile:water (40:60) until 15 min. The detection wavelength was 270 nm for parathion and paraoxon, and 320 nm for 4-nitrophenol, and the injection volume was 100 μl.

The ionic byproducts from parathion degradation were analyzed using a DX-120 ion chromatograph (Dionex). The column was an Ionpac AS14 (Dionex) for NO_2^-, NO_3^-, PO_4^{3-} and SO_4^{2-} analyses, and an Ionpac CS 12-A column (Dionex) for the NH_4^+ analysis. The flow rate was 1 l/min and the injection volume was 25 μl of the filtered reaction samples. The eluent consist of a mixture of 3.5 mM Na_2CO_3 and 1 mM $NaHCO_3$ for the anion analysis, and 20 mM methane sulfonic acid for the cation analysis. TOC analysis was performed with a TOC-5000A analyzer (Shimadzu) using the combustion/non-dispersive infrared gas analysis method calibrated with standard solutions of hydrogen potassium phthalate.

2.4. Toxicity test

The acute toxicity assays using a microbe *V. fischeri* and a macro-invertebrate *D. magna* were performed at different stages of parathion degradation to evaluate the reduction of toxicity throughout the treatments. Standardized test procedures for *V. fischeri* and *D. magna* were employed (Microbics Corp., 1992; US EPA, 2002). The Microtox® Model 500 toxicity analyzer was used to conduct the Microtox assay, and the 81.9% test protocol was followed (Microbics Corp., 1992). The bacteria were exposed to a series of sample dilutions for 5 and 15 min at 15 °C, and then their alteration in light output was measured. All details of the acute toxicity test using daphnids were in accordance with the US EPA acute whole effluent toxicity (WET) test method (2002). Water quality parameters such as pH, temperature, dissolved oxygen, and specific conductivity of the test solutions and control were measured and recorded daily during the testing period.

Lyophilized *V. fischeri*, the test organism for the Microtox assay, was purchased from a commercial vendor (SDI, Newark, DE, USA). The invertebrate test organism, *D. magna*, was cultured in-house. Standard reference toxicity testing was routinely carried out to assure comparable sensitivities of the test invertebrates over time.

3. Results and discussion

3.1. Comparison of parathion degradation between photolysis and photocatalysis

To confirm the role of TiO_2 in the photocatalysis reaction, four sets of experiments were performed to compare parathion degradation rates with and without TiO_2 catalysts. The first set was performed as a blank containing only parathion (10 mg/l). The second set was performed with parathion (10 mg/l) exposed to TiO_2 (1 g/l), but no UV (TiO_2-only condition). The third set was performed by exposing parathion (10 mg/l) to UV without TiO_2 (photolysis condition). Then, the fourth set exposed parathion to TiO_2 (1 g/l) in the presence of UV illumination (photocatalysis condition). The results are presented in Fig. 2.

The blank experiment in the absence of UV and TiO_2 showed that no parathion concentration change for 150 min, which was the longest reaction time of any subsequent experiment. This experiment confirmed no loss of parathion to unknown mechanisms. Next, the experiment with TiO_2-only showed a rapid loss of approximately 10% of the parathion and a constant concentration for the remainder of the test. The disappearance is mostly likely due to adsorption to the TiO_2 particles, which is consistent with expectations since similar results with TNT and other compounds with TiO_2-only have been observed previously in our lab (Son et al., 2004) and by others (Bekkouche et al., 2004). The photolysis reaction degraded approximately 83% of the parathion concentration after 150 min, whereas the parathion was completely removed after 60 min in the photocatalytic reaction. Several studies have shown that photolysis and photocatalysis involve the same

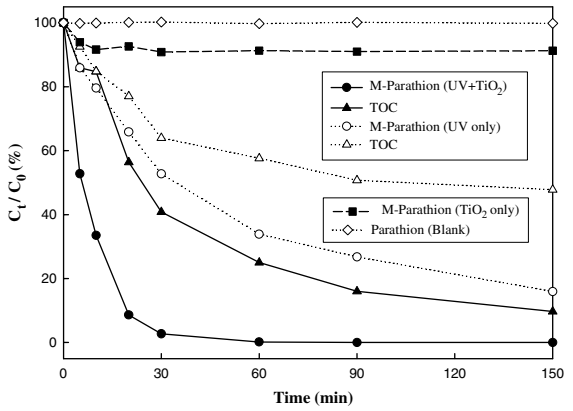

Fig. 2. Degradation of parathion and TOC reduction under the control conditions ([parathion]: 10 mg/l, TiO_2: 0 g/l in the blank and UV only condition, TiO_2: 1.0 g/l in the TiO_2-only and UV + TiO_2 conditions).

degradation pathway, and the difference in the reaction rates between the two processes is due to the hydroxyl radical concentration (Goutailler et al., 2001).

During the photocatalytic degradation of parathion, the pH decreased from 6.5 to 3.8. During photolysis the pH only decreased to 4.5. The pH drop with parathion degradation can be explained by two reactions: a decrease in the concentration of hydroxide ions (OH^-) to produce hydroxyl radicals, and the production of low-molecular-weight organic acids during the oxidation of parathion such as dimethyl phosphoric acid and dimethylthio phosphoric acid (Doong and Chang, 1998).

3.2. Effect of the initial parathion concentration

The pollutant concentration is a very important parameter in its treatment; therefore, the effect of the initial parathion concentration on the photocatalytic degradation rate was investigated from 5 to 20 mg/l. This was well below the solubility of parathion (55–60 mg/l at 25 °C; WHO, 1993), and was sufficiently high to allow the degradation products to be observed by HPLC. Fig. 3(a) shows that the degradation rate decreased with the initial parathion concentration.

The Langmuir–Hinshelwood kinetic expression has been used for TiO_2 photocatalysis to describe the relationship between the initial degradation rate and the initial concentration (Mills and Hoffmann, 1993; Chen and Raym, 1998; Son et al., 2004). In this model, the reaction rate for the second-order surface decomposition of parathion is written as follows:

$$\text{rate} = -\frac{dC}{dt} = k_c \frac{K}{1 + KC_0} C = k_{obs} C \quad (1)$$

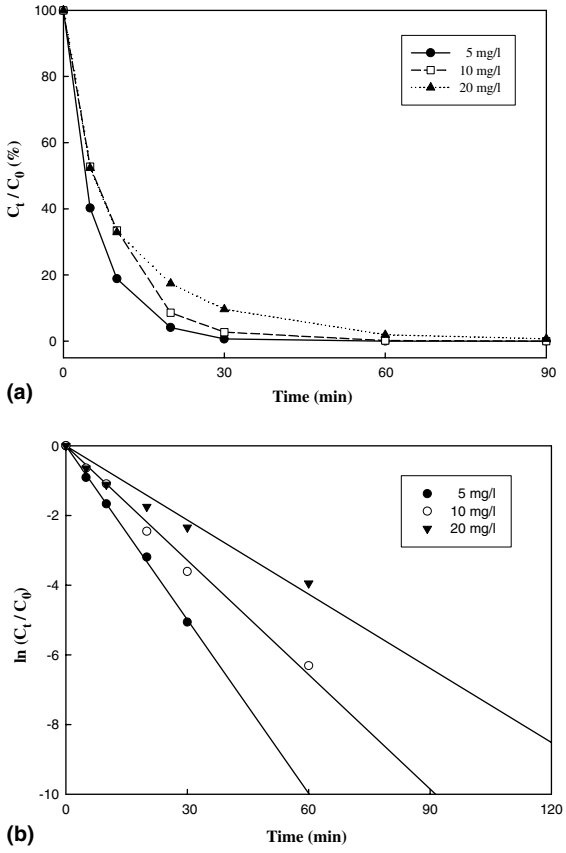

Fig. 3. Effect of the initial parathion concentration on the (a) parathion degradation and (b) pseudo-first-order kinetics under photocatalysis (TiO_2: 1.0 g/l).

where C is the parathion concentration at time t, k_c is the second-order rate constant, K is the equilibrium adsorption constant of parathion onto TiO_2, C_0 is the initial concentration of parathion, and k_{obs} the observed pseudo-first-order rate constant. According to Eq. (1), the photocatalytic degradation of parathion in the presence of TiO_2 should exhibit pseudo-first-order kinetics with respect to the parathion concentration. The integration of Eq. (1) results in Eq. (2):

$$\ln\left(\frac{C_0}{C}\right) = k_{obs} t \quad (2)$$

A straight-line relationship between $\ln(C_0/C)$ and irradiation time is predicted by Eq. (2) and this was observed as indicated in Fig. 3(b). The k_{obs} (min^{-1}) at initial parathion concentration of 5, 10, 20 mg/l was found to be 0.167 ($R^2 = 0.998$), 0.110 ($R^2 = 0.993$), 0.071 ($R^2 = 0.973$) min^{-1}, respectively. These data indicate that the parathion degradation does not follow simple first-order kinetics, but pseudo-first-order kinetics based on the Langmuir–Hinshelwood kinetics.

3.3. Formation of ionic byproducts and mineralization

Since parathion is a phosphorothioate insecticide containing a nitro group and sulfur and phosphorus atoms, NO_2^-, NO_3^-, PO_4^{3-}, and SO_4^{2-} are potential ionic degradation byproducts (Konstantinou and Albanis, 2003). Therefore, we measured the ionic byproducts produced during photolysis and photocatalysis. Fig. 4(a) shows the ionic byproducts during photocatalysis while Fig. 4(b) shows the result with photolysis only.

Fig. 4(a) shows that almost all of the nitrogen was recovered as either NO_3^- or NH_4^+. The concentration of NO_2^- initially increased to 20% of the initial nitrogen present in parathion and then decreased; the maximum NO_3^- concentration was reached when the NO_2^- concentration decreased to zero. In the end, about 80% of the total nitrogen initially present in the parathion was converted to NO_3^-, while about 18% was converted to NH_4^+. Therefore, the predominant nitrogen product is NO_3^-, indicating that oxidation is the principal mode of photocatalytic degradation of parathion. The observed kinetics can be explained by NO_2^- being first cleaved from the parathion molecule during the photocatalytic reaction, and then being rapidly oxidized to NO_3^- by hydroxyl radical attack. Others have observed the conversion of NO_2^- to NO_3^- by a hydroxyl radical in AOP processes (Low et al., 1991; Zoh and Stenstrom, 2002).

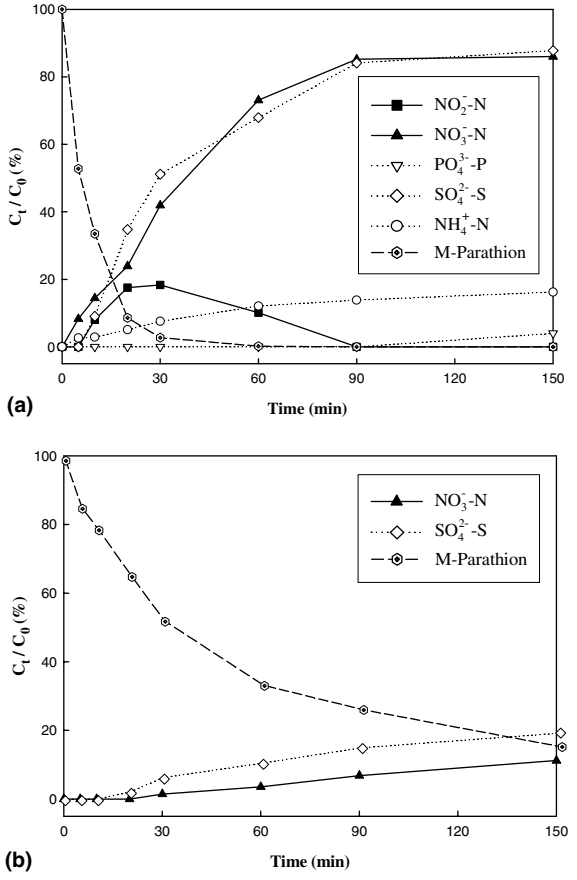

Fig. 4. Degradation of parathion and the formation of ionic byproducts under (a) photocatalysis and (b) photolysis ([parathion]: 10 mg/l, TiO_2: (a) 1.0, (b) 0 g/l).

About 18% of the NH_4^+ was also produced at the end of photocatalysis, as shown in Fig. 4(a). The formation of NH_4^+ indicates that there is a concurrent reduction reaction during the photocatalytic degradation of parathion. According to Piccinini et al. (1997), an electron (e_{CB}^-) can reduce a nitro group to an amine. The resulting amine group can be detached from the benzene ring by a hydroxyl radical.

Sulfate was also rapidly produced, and the total sulfur recovery was 80%. This result indicates that oxidation attack of the hydroxyl radical on the P=S bond first occurred, resulting in the formation paraoxon and sulfate (Konstantinou et al., 2001). The formation of PO_4^{3-} was only observed after 90 min of the photocatalytic reaction, indicating that PO_4^{3-} is the last ionic byproduct of parathion degradation. The continuous attack of the hydroxyl radical followed by the breakage of the P=O bond likely resulted in the formation of 4-nitrophenol and PO_4^{3-}.

In contrast to the photocatalysis reaction, the parathion destruction was much lower and the total amount of nitrogen byproducts produced in the photolysis of parathion was much lower than that produced by photocatalysis. As shown in Fig. 4(b), the NO_3^- produced by the photolysis reaction, while still the major byproduct, represented only 18% of the nitrogen associated with the degraded parathion. Only 24% of the reacted sulfur was recovered as SO_4^{2-}. This phenomenon can be explained by the much lower hydroxyl radical concentration in photolysis versus photocatalysis.

3.4. Formation of organic intermediates

Due to the unavailability of labeled ^{14}C-parathion, TOC measurements were performed to provide indirect evidence of mineralization during the parathion photolysis and photocatalysis experiments. The results are shown in Fig. 2. Approximately 90% of the parathion was mineralized within 150 min by the photocatalytic reaction, while only approximately 52% was mineralized by photolysis alone. The low conversion of TOC by photolysis is believed to be caused by the organic byproducts of parathion.

In order to confirm the mineralization during parathion photocatalysis, the organic byproducts were measured. Paraoxon is a likely organic byproduct, which inhibits the action of acetylcholinesterase (AChE) (La-Grega et al., 2001). Since paraoxon and 4-nitrophenol were previously found to be two major intermediates

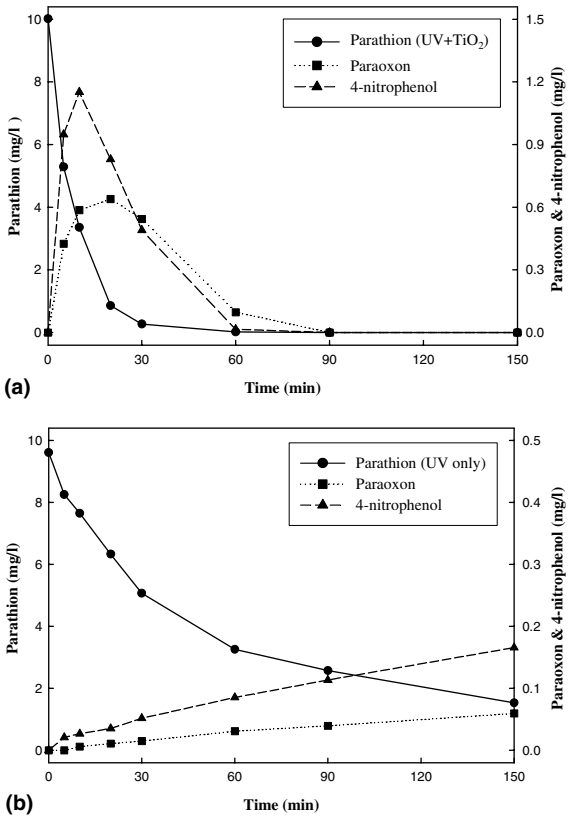

Fig. 5. Photocatalytic degradation of parathion and the formation of organic intermediates with (a) photocatalysis and (b) photolysis ([parathion]: 10 mg/l, TiO_2: (a) 1.0, (b) 0 g/l).

in the photocatalysis of parathion (Konstantinou et al., 2001), these two byproducts were measured during photocatalysis and photolysis.

Fig. 5(a) shows the formation of organic intermediates during the degradation of parathion in photocatalytic treatment. The production pattern of paraoxon and 4-nitrophenol suggest that they are intermediates in the degradation, and is consistent with the hypothesis that the sulfate is produced by the oxidation attack of the hydroxyl radical on the P=S bond, creating paraoxon. Paraoxon undergoes further oxidative attack to produce 4-nitrophenol, which is eventually mineralized through further oxidation. Fig. 5(a) shows roughly 1.2 mg/l paraoxon and 0.63 mg/l 4-nitrophenol were the highest concentrations produced during photocatalytic degradation and occurred in the first 30 min. The maximum recovery of carbon in the photocatalysis was less than 30%.

In the photolysis reaction, only trace amounts of the organic intermediates were produced, as shown in Fig. 5(b). Another difference in the production pattern between photolysis and photocatalysis is that the concentration of intermediates did not decrease, but increased steadily to about 0.07 mg/l paraoxon and 0.17 mg/l 4-nitrophenol after 150 min of photolysis.

3.5. Comparison of acute toxicity and TOC reduction

Numerous studies have examined the photocatalytic degradation of organic contaminants in water, while few have investigated the toxicity profile during the course of photocatalytic degradation (Fernandez-Alba et al., 2002). A wide range of reaction intermediates, which might be more toxic than the parent molecule, could be generated. In this study, less than 30% of the carbon was recovered in the organic intermediates from the photocatalytic degradation of parathion, and an even smaller amount of carbon was observed in the

Table 1
The results of (a) the Microtox test and (b) the 48-h acute *D. magna* toxicity test on the reaction samples treated with photocatalysis and photolysis

Reaction time (min)	EC_{50} (%)					
	0	5	10	30	90	150
(a)						
$UV + TiO_2$ (photocatalysis)	4.31 (3.98–4.68)	7.76 (7.76–7.94)	14.36 (12.70–16.23)	>81.9	>81.9	>81.9
UV-only (photolysis)	4.59 (4.36–4.83)	5.64 (4.85–6.54)	5.67 (5.47–5.87)	8.46 (7.74–9.24)	18.26 (17.64–18.91)	29.48 (26.36–32.97)

	EC_{50} (%)			
	0	30	90	150
(b)				
$UV + TiO_2$ (photocatalysis)	0.05 (0.04–0.06)	0.07 (0.06–0.09)	21.02 (17.70–24.99)	25.00 (21.48–29.10)
UV-only (photolysis)	0.04 (0.04–0.06)	0.10 (0.08–0.11)	0.14 (0.12–0.17)	0.13 (0.11–0.15)

photolytic reaction. This indicates the possibility of unknown byproducts from the reaction. Therefore, it is necessary to investigate the toxicity of the treated solution at different illumination times.

In order to test the reduction of toxicity during the photocatalytic and photolytic degradation of parathion, two acute toxicity tests were conducted: a modified Microtox® 81.9% test using *V. fischeri*, and a 48-h acute toxicity test using *D. magna*. The reduction in acute toxicity during the reactions was compared with the pattern of parathion degradation and TOC mineralization.

Table 1 shows the Microtox test results using *V. fischeri* during the photocatalysis and photolysis reactions. Table 1 indicates that the EC_{50} (%) increased from 4.31% to more than 81.9% during photocatalytic degradation, showing that the acute toxicity disappeared. Under photolysis, the EC_{50} (%) of the reaction solution increased from 4.59% to 29.48% at 150 min, and the samples remained toxic.

Another acute toxicity test was conducted using *D. magna*, and the results are also summarized in Table 1. Table 1 shows that the EC_{50} (%) increased from about 0.05% to more than 25% during photocatalytic degradation. However, the EC_{50} (%) of the reaction solution increased from 0.04% to only 0.13% at 150 min using photolysis, indicating that almost no detoxification occurred.

To further illustrate the reduction in toxicity, the relative toxicity (%) during the photocatalytic and photolytic degradation of parathion using the EC_{50} (%) values in Table 1 was plotted against illumination time, and is shown in Fig. 6.

Relative toxicity can be expressed as follows:

$$\text{relative toxicity } (\%) = \frac{\text{initial } EC_{50}\ (\%)}{\text{observed } EC_{50}\ (\%)} \times 100 \qquad (3)$$

The TOC profiles are overlaid on the graphs to demonstrate the relationship between relative toxicity (%) and TOC concentration. Careful examination of the TOC and toxicity profiles reveals that as both the TOC and parathion concentrations decreased as the reaction proceeded, there was a significant decrease in the acute toxicity.

Fig. 6(a) shows that the complete removal of parathion and a 90% reduction in TOC during photocatalysis was responsible for the almost complete disappearance of acute toxicity in *V. fischeri* and *D. magna* bioassay during the reaction. Under photolysis, the relative toxicity decreased to 65% in *D. magna*, and 83% in *V. fischeri* while 83% of the parathion and 52% of the TOC were removed, as shown in Fig. 6(b). These results indicate that TOC is a parameter that can easily be correlated with toxicity, and the intermediates produced from parathion degradation are less toxic for *V. fischeri* and *D. magna* than the parent compound.

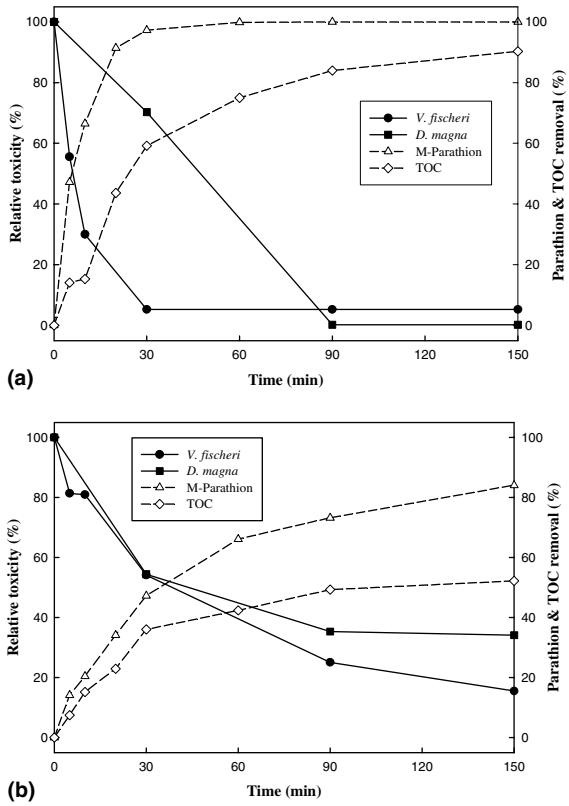

Fig. 6. Comparison between acute toxicities reduction (*V. Fischeri* and *D. magna*) and parathion and TOC degradation under (a) photocatalysis and (b) photolysis ([parathion]: 10 mg/l, TiO_2: (a) 1.0, (b) 0 g/l).

The acute toxicity analyses showed that in all cases, especially photocatalysis, the products of the reactions were less toxic for *V. fischeri* and *D. magna* than the original solution containing parathion. The analyses also revealed that *D. magna* is a more sensitive indicator for parathion than *V. fischeri*.

4. Conclusions

This study examined the efficacy of the photocatalytic degradation of parathion by TiO_2/UV photocatalysis. The conclusions were as follows:

1. The rate of parathion degradation decreased with an increasing initial concentration of parathion, and the degradation kinetics followed pseudo-first-order kinetics based on the Langmuir–Hinshelwood kinetics.
2. Photocatalysis was effective in degrading parathion and was much more effective than photolysis. TiO_2 without UV light was ineffective and only 10% of the parathion was removed by adsorption onto the

TiO_2 particles. The percent degradation of parathion under photocatalysis and photolysis for 150 min was 100% and 83%, respectively. In the same period, the % decrease in TOC was 90% and 47%, respectively.

3. Paraoxon and 4-nitrophenol were found to be the intermediates and disappeared completely after 90 min under photocatalysis, but never disappeared using photolysis.
4. NO_3^- and SO_4^{2-} were the dominant byproducts, and the formation of PO_4^{3-} was observed under photocatalysis.
5. The Microtox test using *V. fischeri* showed that EC_{50} (%) was completely eliminated with photocatalysis, but was reduced only 83% after 150 min of photolysis. The acute 48-h toxicity test using *D. magna* was more sensitive and also showed that the relative toxicity disappeared after 90 min under photocatalysis, whereas there was a 65% reduction with photolysis alone. The pattern of toxicity reduction parallels the decrease in TOC and the parathion concentrations.

These results show that the parathion degradation using photocatalysis not only removed the parathion and its intermediates, but also decreased their toxicity.

Acknowledgment

This work was supported by the Korea Research Foundation Grant funded by the Korean Government (MOEHRD) (KRF-2003-003-D00217).

References

Bekkouche, S., Bouhelassa, M., Hadj Salah, N., Meghlaoui, F.Z., 2004. Study of adsorption of phenol on titanium oxide (TiO_2). Desalination 166, 355–362.

Chen, D., Raym, A.K., 1998. Photodegradation kinetics of 4-nitrophenol in TiO_2 suspension. Water Res. 32, 3223–3234.

Doong, R.A., Chang, W.H., 1998. Photodegradation of parathion in titanium dioxide and zero valent iron solutions in the presence of hydrogen peroxide. J. Photochem. Photobiol. A: Chem. 116, 221–228.

Dzyadevych, S.V., Chovelon, J.M., 2002. A comparative photodegradation studies of methyl parathion by using Lumistox test and conductometric biosensor technique. Mater. Sci. Eng. C 21, 55–60.

Fernandez-Alba, A.R., Hernando, D., Aguera, J., Caceres, J., Malato, S., 2002. Toxicity assays: a way for evaluating AOPs efficiency. Water Res. 36, 4255–4262.

Germain, A., Bizzarri, D., Dodet, C., 2000. Thermal decomposition of ethyl and methyl parathion. J. Loss Prevent. Process Indust. 13, 15–22.

Goutailler, G., Valette, J.C., Guillard, C., Paisse, O., Faure, R., 2001. Photocatalyzed degradation of cyromazine in aqueous titanium dioxide suspensions: comparison with photolysis. J. Photochem. Photobiol. A 141, 79–84.

Konstantinou, I.K., Albanis, T.A., 2003. Photocatalytic transformation of pesticides in aqueous titanium dioxide suspensions using artificial and solar light: intermediates and degradation pathways. Appl. Catal. B: Environ. 42, 319–335.

Konstantinou, I.K., Sakellarides, T.M., Sakkas, V.A., Albanis, T.A., 2001. Photocatalytic degradation of selected s-triazine herbicides and organophosphorus insecticides over aqueous TiO_2 suspensions. Environ. Sci. Technol. 35, 398–405.

LaGrega, M.D., Buckingham, P.L., Evans, J.C., 2001. Hazardous Waste Management, second ed. McGraw-Hill, New York.

Low, G., McEvoy, S.R., Stephan, M.A., Matthews, R.W., 1991. Formation of nitrate and ammonium ions in titanium dioxide mediated photocatalytic degradation of organic compounds containing nitrogen atoms. Environ. Sci. Technol. 25, 460–467.

Malato, S., Blanco, J., Campos, A., Cacers, J., Guillard, C., Herrmann, J.M., Fernandez-Alba, A.R., 2003. Effect of operating parameters on the testing of new industrial titania catalysts at solar pilot plant scale. Appl. Catal. B: Environ. 42, 349–357.

Microbics Corp., 1992. Microtox™ Manual: A Toxicity Testing HandbookDetailed Protocols, vol. II. Microbics Corp., Carlsbad CA, USA.

Mills, G., Hoffmann, M.R., 1993. Photocatalytic degradation of pentachlorophenol on TiO_2 particles—identification of intermediates and mechanisms of reaction. Environ. Sci. Technol. 27, 1681–1689.

Piccinini, P., Minero, C., Vincenti, M., Pelizzetti, E., 1997. Photocatalytic interconversion of nitrogen-containing benzene derivatives. J. Chem. Soc., Faraday Trans. 93, 1993–2000.

Schulz, R., Moore, M.T., Bennett, E.R., Milam, C.D., Bouldin, J.L., Farris, J.L., Smith Jr., S., Cooper, C.M., 2003. Acute toxicity of methyl parathion in wetland mesocosms: assessing the influence of aquatic plants using laboratory testing with Hyalella azteca. Arch. Environ. Contam. Toxicol. 45, 331–336.

Son, H.S., Lee, S.J., Cho, I.H., Zoh, K.D., 2004. Kinetics and mechanism of TNT degradation in TiO_2 photocatalysis. Chemosphere 57, 309–317.

US EPA, 2002. Method for Measuring the Acute Toxicity of Effluents and Receiving Water to Freshwater and Marine Organisms, fifth ed. EPA/821/R- 02/012, Office of Research and Development, Washington DC, USA.

US EPA (Ired signed 05/2003). Interim registration eligibility document for methyl parathion.

WHO, 1993. Environmental health criteria for methyl parathion, 145, WHO, Geneva, Switzerland.

WHO, 2004. WHO Guidelines for Drinking-Water Quality, third ed. World Health Organization (WHO/SDE/WSH/03.04/110), Geneva.

Zoh, K.D., Stenstrom, M.K., 2002. Fenton oxidation of hexahydro-1,3,5-trinitro-1,3,5-triazine (RDX) and octahydro-1,3,5,7-tetranitro-1,3,5,7-tetrazocine (HMX). Water Res. 36, 1331–1341.